IDENTIFICATION OF PHOSPHORUS LOSS SPATIAL FEATURES IN TYPICAL LAND USE PATTERNS COUPLED WITH REMOTE SENSE AND SOIL ANALYSIS

C. Lin, R.H. Ma

ABSTRACT. *The soil phosphorus (P) assessment is of great significance for agricultural non-point source pollution management in watersheds. Many of current studies provided data with limited accuracy and at relatively small spatial scale, due to the low spatial resolution of available remote sense data. This study used solid pollutants loss equation and high-resolution remote sense data source to determine the spatial characteristics of P loss, and then identified the critical polluted areas and corresponding underlying surface conditions within each land use type. Results showed that non-eroded region and slightly loss region covered more than 65% of the entire area. Although the severely-eroded region only accounted for 12.8% of the area, this region was distributed in the vicinity of downstream of two major inflow drainages. Hence, the harmful effect of this region on the watershed environment should not be neglected. The P loss varied significantly among different land use types, including forest land, arable land and orchard land. The forestland exhibited the lowest loss intensity, while the arable land exhibited the highest loss intensity. And the variation degree of P loss intensity within orchard land was probably greater than the other two land use patterns. Furthermore, this diversity in P loss largely resulted from different underlying surface features including topography, vegetation status, and key soil properties. The result from this study is suitable for practical use in different management strategies for non-point source pollution (NPS) management.*

Keywords. *Non-point source pollution, Remote sense, Soil Phosphorus, Spatial characteristics.*

Phosphorus (P) is an essential element for crop growth, and a primary nutrient of eutrophication of aquatic ecosystem (Norton et al., 2012). In recent decades, soil P loss via agricultural non-point source (NPS) pollution in watershed has been recognized as a severe threat to the aquatic environment, and a significant portion (80%) of P loss was in a particulate form (PP) (Evanylo et al., 2008; Castoldi et al., 2009). Therefore, the accurate evaluation of PP loss in watersheds and the identification of critical polluted areas (CPAs) are of great significance for the management of NPS pollution (Yang, 2009).

Soil P loss occurs through a complex hydrological processes and is influenced by various anthropogenic and geographical factors, including land use, soil erosion, agricultural fertilization, atmospheric conditions, hydrological factors, etc. Although a large number of physical and exponential models have been developed to identify and quantify the main factors responsible for PP loss from NPSs, including SWAT (Laurent and Ruelland, 2011); ANSWERS (Beasley et al., 1980), solid pollutants loss model (Wang et al., 2012), and APPI (Gburek and Sharpley, 1998; Shen et al., 2011), many of them are physics-based models, use complex parameters, and rely on detailed field observations, causing them unsuitable at-large spatial scales due to high cost of field observation (McDowell et al., 2002). Compared with physical models, the classical empirical models are more suitable and widely used in watershed scale monitoring due to the advantages of condensed structures, accessible parameters, and simple and efficient operation (Bechmann et al., 2009; He et al., 2012). In particular, the most recognized exponential model is the Revised Universal Soil Loss Equation (RUSLE), which has been widely applied to evaluate soil erosion modulus by integrating several factors, including climate, land use, soil and topography (Ouyang et al., 2010; Ouyang et al., 2012; Yang et al., 2012). Based on the fundamental form of RUSLE, the sediment delivery distributed (SEDD) model has been recently improved by researchers. One of the improvements is to take the sediment delivery factor and soil P status factor into account, and thereby, the loss of the absorbed nutrients in soil sediment can be quantitatively and more precisely monitored (Fu et al., 2006; Jain and Kothyari, 2000). In addition, the spatial information of some modeling factors including land use, vegetation coverage, elevation, slope and surface temperature can be captured efficiently using geography information system science (GIS) and remote sense (RS) technology, which can further simplify the model

Submitted for review in February 2015 as manuscript number ITSC 11247; approved for publication by the Information, Technology, Sensors, & Control Systems Community of ASABE in March 2016.

The authors are **Chen Lin,** Assistant Professor, and **Ronghua Ma,** Professor, State Key Laboratory of Watershed Geographic Sciences, Nanjing Institute of Geography and Limnology, Chinese Academy of Sciences, Nanjing, China. **Corresponding author:** Chen Lin, 73 East Beijing Road, Nanjing 210008, China; phone: +86-25-86882169; e-mail: clin@niglas.ac.cn.

processing (Sridhar et al., 2009; Cheng et al., 2012; Emili and Greene, 2013). Currently, the RUSLE and SEDD models have been applied in several major freshwater lake watersheds in China, such as Chaohu and Taihu Lake watershed (Zhou and Gao, 2008).

However, this approach also has some limitations. The first limitation is land use data source. The spatial distribution of land use is critical to the solid pollutants loss model, in which many model factors including soil erodibility, soil and water conservation factor were needed for the calculation. Many previous studies interpreted the land use from low-medium spatial resolution data sources that are only supposed to be suitable for large-scale research. The spatial data resolution is not fine enough for small spatial-scale analysis because the existence of mixed pixels always results in inaccurate identification of some typical land use types such as forestland and orchard land (Li et al., 2007). For this case, the high spatial resolution remote sense data are needed at relative small spatial scale, especially for some typical sub-catchments. The second limitation is soil P data. Soil P concentration is an important model factor, and is basically assigned by the background P level of each soil type. However, as the land use type and cropping patterns are transformed dramatically in recent decades, soil properties have been changed greatly. Therefore, the field sampling based on different land use and soil types may be needed to more accurately evaluate the current status of soil P (Zhang et al., 2013). Therefore, further improvement is needed in the spatial accuracy of soil P loss in small spatial scale.

The watershed of Meiliang Bay has experienced the most severe eutrophication level within the Taihu Lake. The watershed area covered 486.2 km^2, where witnessed significant land use change and cropping pattern adjustment in recent 30 years due to rapid economic growth in this area, resulting in a substantial increase of non-point source pollution and soil PP loss. Therefore, the objectives of the present study were: i) to evaluate spatial characteristics of soil PP loss using solid pollutants loss model and high-resolution remote sense data source; ii) to extract and identify critical polluted areas and corresponding underlying surface conditions within selected typical land use patterns (forestland, arable land, and orchard land). The results of this study should be applicable to the management of NPS pollution.

Material and Methods

The Study Area

The Meiliang Bay has experienced severe eutrophication level within Taihu Lake, China. The watershed region of Meiliang Bay is located in China's eastern coast, south of the Yangtze River Delta. The area covered 456.2 km^2, and this region is located in a peri-urban area between Wuxi, Changzhou city, which are famous for its natural conditions and advantageous economic development with most extensive agricultural, urban, and industrial areas in the Jiangsu province. The study area is undergoing the dramatic land use adjustment and rapid urbanization in recent 30 years, a large number of arable land and forestland was replaced by construction land. The average annual precipitation at the study site is 1035 mm, and the main rainfall season is from May to October, and the annual mean runoff depth is 688 mm and the annual average temperature is 15.6°C. The main soil type is bleached paddy soil, which covered more than 85% of the entire study site (Gong et al., 2003; Li et al., 2007). Moreover, the sub-watershed is densely covered by water network consisting of three trunk streams with their tributaries such as Wujin Port and Yangxi Rivers which flows into Meiliang Bay of Taihu Lake. Sixteen sub-basins were generated by ArcGIS 10.0 (ESRI) based on the three inflow rivers, in which the Hydology module of Spatial Analyst Tools were applied (fig.1)

Land Use Classification by High-Resolution Remote Sense Data

Land use map in 2012 was interpreted from Resource Satellite ZY-3 image, this Resource Satellite was launched on 9 January 2012. The image product was integrated with

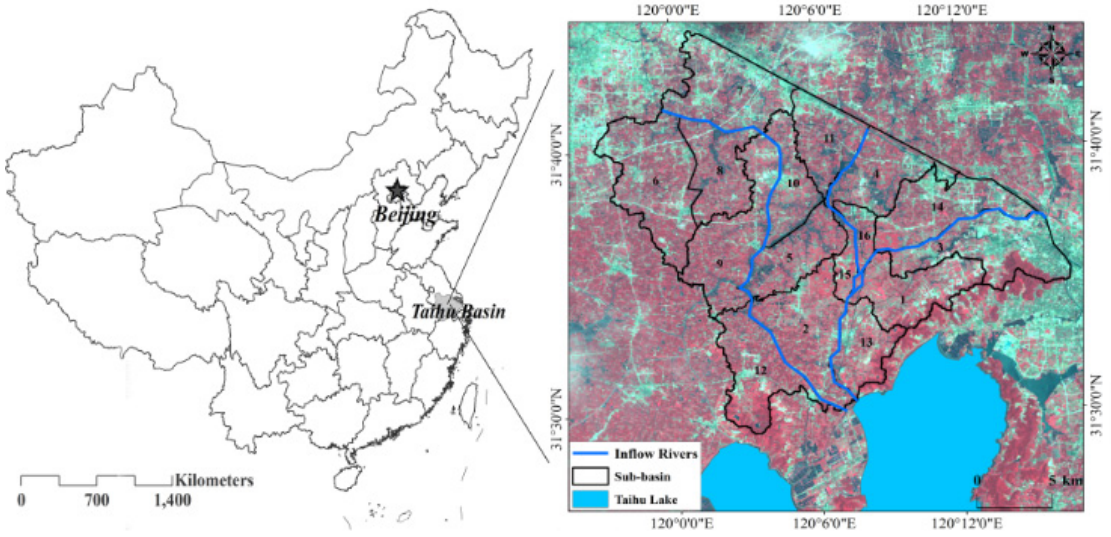

Figure 1. Location of study site.

four multi-spectral bands that covered the spectral region from 0.45 to 0.89 μm, which owned the spatial resolution of 2.1 m. The land use data product was developed in the Data Center for Geography and Limnology Science, Chinese Academy of Science in Nanjing, China. Before the classification, the data preprocessing such as atmospheric correction and geometric correction were conducted by Envi (The Environment for Visualizing Images) #5.0, a remote sensing image processing software. And then the object oriented interpretation was carried out to create land cover maps by eCognition #8.0, which is an intelligent image analysis software. Finally, the interpretation results were validated by field work, which was organized by the Institute of Geographic Sciences and Natural Resources Research Chinese Academy of Science in Beijing, China (75 actual survey points were located in the study site of this study, the field points were used to compare the actual land use pattern with the interpreted land use pattern), and there are 68 samples owned with the consistent land use pattern, which showed that the overall users accuracy reached 90.7%. This study focused on three typical land use patterns: orchard land, forestland and arable land. During the interpretation process, some more detailed land use patterns were identified, and these patterns were clustered into the three land use types to simplify the research. Figure 2 shows the land use map of 2012.

Soil Sampling and Measurements

In order to assess the current status of PP and provide basis for pollutants loss model, the field sampling and investigation was conducted. The study area was divided into three sections based on selected typical land use patterns, and total of 75 soil samples were collected uniformly in the study site (fig. 2). The soil samples were air dried and ground prior to chemical analysis.

Basic soil properties were measured in State Key Laboratory of Soil and Sustainable Agriculture, Chinese Academy of Science in Nanjing, China. Some other critical soil physicochemical parameters such as soil organic matter (SOM), total phosphorus (TP), total nitrogen (TN), available P (Olsen-P), and soil texture with composition of sand, silt, and clay were also measured. To measure the TN and TP, soil samples were digested with HNO_3–HF–$HClO_4$. To determine Olsen-P (available P), 1 g air-dry soil (sieved < 2 mm) was shaken in 20 mL 1 M sodium hydrogen carbonate, ($NaHCO_3$, pH 8.5) for 30 min (Osborne et al., 2002; Lin et al., 2008), and the supernatant was measured for P concentration. The soil organic matter (SOM) of each sample was determined after oxidation using potassium dichromate ($K_2Cr_2O_7$) and sulphuric acid (H_2SO_4), and also measured by external heating method (Houba et al., 1989). The contents of sand (0.05 to 2 mm), silt (0.002 to 0.05 mm) and clay (0 to 0.002 mm) particles in soil were measured using pipette method (Soil Science Society of China, 2000).

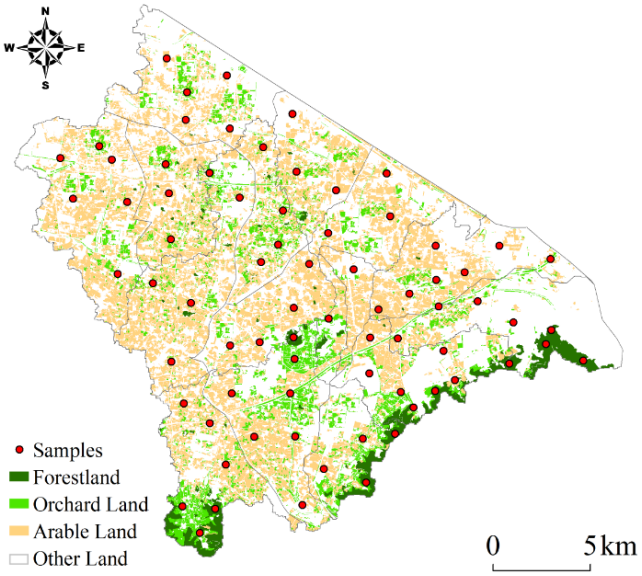

Figure 2. Spatial distribution map of land use patterns and soil samples.

Calibration and Validation of Pollutants Loss Model

The solid pollutant loss model should include three key modules: soil erosion, content of P and sediment transport. The SEDD model, which is optimized based on the fundamental form of Revised Universal Soil Loss Equation (RUSLE), has the capability to incorporate the P concentrations and sediment delivery ratio, in addition to the factor of soil erosion. (Cui et al., 2003; Yang et al., 2012). The model was calculated in ArcGIS using 30 × 30 m spatial grids:

$$Par(P) = A_i \times P_{sed} \times SDR_i \quad (1)$$

where $Par(P)$ is the particulate P loads per unit area ($t \cdot km^{-2} \cdot yr^{-1}$); P_{sed} expresses the sediment total P concentration status ($g \cdot kg^{-1}$); SDR_i is the sediment delivery ratio (%) for each grid, A_i is the soil erosion modulus ($t \cdot km^{-2} \cdot yr^{-1}$).

P_{sed} were assigned based on different sub-basins and land use types, the runoff samples were obtained after typical rainfall events based on three lane use patterns for different sub-basin, and each sample were corresponding to certain land use pattern for different sub-basins. Surface runoff samples were filtered through a 0.7-μm porosity, precombusted glass fiber filters (25 mm diameter; Whatman GF/F). The particulate phosphorus concentrations were measured in soil and environment analysis center, Institute of Soil Science, Chinese Academy of Sciences, and analyzed with inductively coupled plasma-atomic emission spectrometry (ICP-AES) (Lin et al. 2008). SDR_i is the sediment delivery ratio (%) for each grid, which is calculated based on the following model:

$$SDR_i = exp(-\beta t_i) \quad (2)$$

where t_i is the travel time (h) from the grid i to the nearest river channel along the flow path and β is a coefficient lumping together the effects of roughness and runoff along the flow path (Ferro, 1997). The β is watershed-specific, and the value of 0.304 is suitable for the Taihu watershed because this value produces smallest mean relative square

error between modeled and measured sediment yield (Guo et al., Strauss et al., 2007). t_i can be calculated based on the equation (3)(Jain and Kothyari, 2000), in which l_j is the flow length and v_j is a velocity factor derived from Smith and Maidment (1995)

$$t_i = \sum_{j=1}^{N_P} \left(\frac{l_j}{v_j} \right) \tag{3}$$

A_i was calculated by RUSLE.

$$A_i = R_i \times K_i \times LS_i \times C_i \times P_i \tag{4}$$

where R_i is the rainfall-runoff erosivity factor [MJ mm· (ha h yr)$^{-1}$]; K_i is the soil erodibility factor (Mg h MJ^{-1}mm^{-1}); LS_i is the slope length and steepness factor; C_i is the cover management factor. Specially, ***R*** was calculated using the formula proposed by Xu et al. (2007): R_i=0.689$P_i^{1.474}$, where R_i is the yearly rainfall erosivity (MJ·mm·km^{-2}· h^{-1}·month^{-1}) and P_i is the monthly precipitation, the averaged values of monitored precipitation for each month were designated as the yearly value. The K value can be calculated by soil properties in different soil types, using the Wischmeier's soil erodibility nomograph (Wischmeier and Smith, 1978; Xu et al., 2012). And in this study, the soil type was assigned by the soil type spatial distribution map (1:1000000), and the K value for each soil type was referenced to the study of Bu et al. (2002), which was conducted in Taihu Basin. The factor *LS* reflects the effects of topography on soil erosion and is the acceleration factor of erosion power. *LS* factors include slope length and steepness factors, which were extracted from ASTER global DEM data, the spatial accuracy was 30 m. *P* is determined as the ratio between the soil losses expected for certain soil conservation practice and usually estimated based on land use type. In this study, the *P* assignment was referenced Xu et al. (2012), which was determined by local investigation in Taihu basin. *C* is defined as the cover-management factor, which express the protective effect of soil cover against the erosive action of rainfall. *C*-factor mapping by remote sensing can provide essential information for improving the spatial modeling of soil erosion (Durigon et al., 2014). In this study, the *C* factor is calculated referenced by Durigon et al. (2014), which involve the use of regression equation derived from correlation analysis between the factor *C* measured in the field and a satellite-derived NDVI. To facilitate the spatial expression and calculation, the non-point particulate P loss modulus were calculated in ArcGIS 10.0 environment for each pixel, and then the spatial distribution feature of *Par*(*P*) were analyzed from sub-basin scale as well as the scale of different land use patterns.

To validate the model, the quantitative measures were used to compare the observed data with the simulated values. The monitoring sites were located in the outlet of each sub-watershed, and they were used to observe the actual sediment and runoff discharge of the sub-watershed under severe rainfall conditions (four times per year, and the averaged values were designated as observed values). The Nash–Sutcliffe coefficient (E_{NS}) was used to assess the performance of the model in this study (Nash and Sutcliffe, 1970), and it is defined as:

$$E_{\mathrm{NS}} = 1 - \frac{\sum_{i=1}^{\mathrm{N}} \left(Q_{obs,i} - Q_{sim,i} \right)^2}{\sum_{i=1}^{\mathrm{N}} \left(Q_{obs,i} - \bar{Q}_{obs} \right)^2} \tag{5}$$

where $Q_{obs,i}$ and $Q_{sim,i}$ are the observed and predicted values, respectively. Q_{obs} is the mean observed values within 18 sub-basins, and the $Q_{sim,I}$ is the mean simulated values within 16 sub-basins. The observed and predicted values for phosphorus and sediment loss within the 16 sub-watersheds with respect to 1:1 line were plotted graphically in figure 3, in which figure 3(a) represented the relationship between observed sediment discharge amount and predicted sediment discharge amount, the figure 3(b) represented the relationship between observed phosphorus loads in sediment and predicted PP loss amount which were calculated by SEDD model. The E_{NS} statistical data for the entirely watershed were demonstrated in table 1.

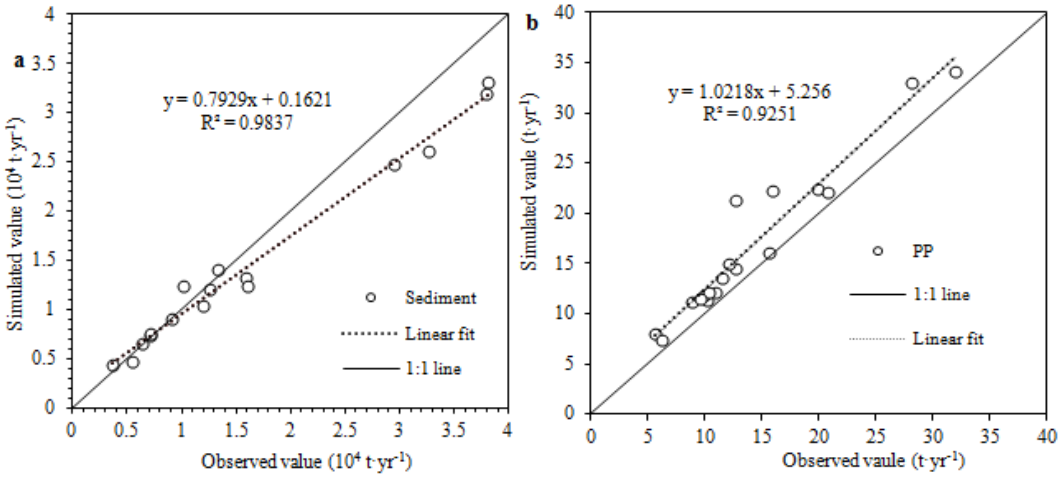

Figure 3. Scatter diagram of observed and predicted values within 18 sub-basins (a) relationship between observed sediment discharge amount and predicted sediment discharge amount; (b) relationship between observed PP loads and predicted PP loss amount.

The figure 3 illustrated that the observed and simulated values for PP and sediment loss amount were distributed uniformly along the 1:1 line. From table 1, the R^2 and E_{NS} were also achieved an ideal score, in which the score of the indicators mentioned in table 1 were reached 0.9 simultaneously. The validation results indicated that the model has simulated accurately the Phosphorus and sediment loss for the watershed for the entire year, and a close agreement between the observed and simulated phosphorus and sediment discharge amounts were also revealed during the model validation.

Analysis of Underlying Surface Conditions under Critical Loss Region

Based on the *Par*(*P*) calibration results, the PP loss status was divided into four grades: non-eroded, slightly loss, moderate loss and severely loss. The classification was executed in ArcGIS 10.0 by Jenks natural break method. The surface features such as vegetation status, topography and soil properties of each grade were analyzed to identify the critical factors of PP loss using discrepancy analysis between different loss grades and land use patterns. Specially, the elevation and slope data were extracted from ASTER global DEM, which were acquired from U.S. Geological Survey (USGS), and the spatial accuracy was 30 m. The normalized differential vegetation index (NDVI) data were extracted from Landsat Enhanced Thematic Mapper (ETM+) data, which were launched by National Aeronautics and Space Administration(NASA), the spatial accuracy was 30 m, and the ETM+ were also sourced from USGS (http://www.usgs.gov/). The satellites transit date were obtained for each month of 2013, the cloud coverage of each satellite image was lower than 10%. And the NDVI value within different months was averaged to represent the NDVI status. Table 2 shows the selected underlying surface indicators. Finally, in order to validate the statistical significance between different eroded groups, the t-tests were introduced into the study. The significance tests were conducted in SPSS 18.0 and the default significant value were designated as 0.05.

Table 1. Goodness-of-fit statistical data for model's validation.

	Annual Mean Yield			
	Observed	Simulated	R^2	E_{NS}
PP ($t \cdot yr^{-1}$)	16.464	14.037	0.925	0.878
Sediment ($10^4\ t \cdot yr^{-1}$)	1.694	1.524	0.984	0.901

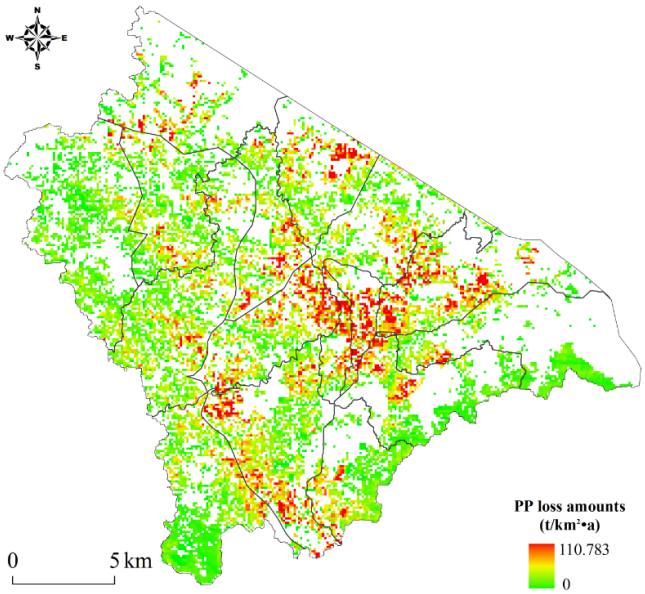

Figure 4. PP loss status assessed by solid pollutants loss equation.

Results and Discussion

The PP Loss Status

Figure 4 shows the general spatial features of PP loss according to the solid pollutants loss model realized in GIS environment. The simulated PP loss amount for the entire watershed ranged from 0-111.783 $t/km^2 \cdot a$. To further understand the spatial features of PP loss status, the statistical results of particulate P loss modulus and the land use configuration within typical sub-basins were shown in table 3. The significance value (*P*) for severely eroded group and slightly eroded group were 0.01(<0.05), which showed that the differences between the two eroded regions meet the significance level.

The results showed: (i) The PP loss mainly occurred in areas of non-eroded grade and slightly eroded grade, which covered 37% and 30% of the entire area, respectively. These two classes accounted for more than 2/3 of the total area. Conversely, none of the areas of mid-eroded and severely-eroded grades exceeded 20%. In general, PP loss condition was not severe in the entire area although some notable spatial heterogeneity existed (fig. 4). (ii) The area of severely-eroded grade comprised only 12.8% of the entire area, which was significantly less than the slightly eroded and mid-eroded grades. However, the severely-eroded region was obviously aggregately distributed in the vicinity of downstream of two major inflow drainages, and the harmful effect of this region on the watershed

Table 2. The data source and assessment method of selected underlying surface indicators.

Indicators	Data Source	Method
Elevation	ASTER global DEM	Extracted by ArcGIS
Slope	ASTER global DEM	Extracted by ArcGIS using 'Slope' tool
NDVI	Landsat Enhanced Thematic Mapper (ETM+) data	Extracted by ArcGIS using 'Raster Calculation' tool Model: (NIR-VIS)/(VIS+NIR)
Soil organic matter(SOM)	Measurement of soil samples	The experimental method was showed above
Soil mechanical composition	Measurement of soil samples	The experimental method was showed above
Soil Total Nitrogen	Measurement of soil samples	The experimental method was showed above

Table 3. Statistical results of PP loss within typical sub-basins (*P<0.05*).

Intensity	Sub-Basin ID	Loss Amount (t/km²•a)				Land Use Composition (%)		
		Min	Max	Mean	SD[a]	Forestland	Arable Land	Orchard Land
Severely	16	0	89.98	33.30	19.32	0.12	72.19	5.32
	15	0	91.56	26.20	18.97	5.12	32.08	16.58
	14	0	88.03	25.44	18.46	0.33	43.02	4.75
Slightly	12	0	58.08	9.24	9.86	15.69	34.23	21.29
	3	0	57.51	9.01	10.04	15.77	12.37	5.71
	6	0	59.46	6.74	6.96	1.79	57.04	6.04

[a] SD: Standard Deviation

environment should not be neglected, due to the this region located at nearby downstream, the pollutants can be discharged into the aquatic environment directly. (iii) The 16th, 15th, and 14th sub-basins experienced with the severest PP loss status, whereas the 12th, 3rd, and 6th sub-basins exhibited the slightest PP loss (table 3). These two regions of severely and slightly loss status had distinctive spatial distribution characteristics; the severely loss region was located and concentrated in the surrounding or in junction of Yangxi River, while the slightly loss region was scattered in the southern edge of the study site. (iv) The mean loss amounts of severe loss sub-basins exceeded 25 t/km²•a, and even reached 33.30 t/km²•a in 16th sub-basin, whereas the amounts in slightly loss sub-basins were less than 10 t/km²•a. In addition, the SD value were also differenced notable between the two groups (18~19 for severely loss region and 6.96~10.04 for slightly loss regions). The results demonstrated that the severely loss status were only appeared in some specific areas within severely loss sub-basins, and the other areas were not eroded severely at all, which resulted in the high spatial variability within the severely loss region.

THE PP LOSS AMONG DIFFERENT LAND USE PATTERNS

Based on the spatial visualization of PP loss, we further analyzed PP loss variation characteristics among three typical land use patterns.

Forestland exhibited the most remarkable differences between the severely loss region and the slightly loss region; the forestland in the slightly loss region was significantly higher than that in the severely loss region. Within the severest loss region, almost no forest land was distributed in 14th and 16th sub-basins, and forestland only occupied 5% of the area in the 15th sub-basin, whereas, the proportion of arable land and orchard land reached approximately 50%, far more than the forestland area in this region. In the slightly loss region, however, forestland coverage reached 15%, which was the highest among sixteen sub-basins. The only exception was 6th sub-basin, which only had 1.79% forestland but exhibited the slightest PP loss, possibly because the sub-basin was apart from the inflowing river and was located on the edge of the study area. These results indicated that various land use types had significant impact on soil PP loss.

Table 4 shows the statistical results related to PP loss among three patterns for the entire study area. The differences of PP loss among three land use types suggested that forestland experienced the slightest PP loss. The average PP loss of the forestland was less than 10 t/km²•a, and some areas showed completely no PP loss at all. Moreover, the non-eroded area and slightest loss area accounted for 97% of the total forestland region, and areas of severely loss rarely appeared. These results indicate that forestland plays a prominent role in watershed conservation. It can enhance the soil stability and alleviate the nutrients loss from agriculture non-point source pollution to some extent. In contrary, the PP loss within arable land and orchard was much more severe than that within forestland. The maximum loss amount of these two land uses exceeded 100 t/km²•a. The differences between these two types were needed to discuss. In general, the PP loss amount of arable land seemed slightly higher than orchard as the maximum and mean values of arable land exceeded those of orchard land (table 4). However, the coefficient of variations of orchard land (49.8%) was higher than arable land significantly. The higher degree of variation coefficient may be due to variety of planting patterns in the orchard land, including tea plantations, peach orchards and citrus orchards. This kind of diversity obviously differentiated from arable land, where was substantially covered by wheat fields in our study (Zhang et al., 2009). The diverse cropping patterns can also lead to variations in the amounts of chemical fertilizer and pesticides used, which most likely leads to the variations of non-point pollution intensity within orchard land (Gburek et al., 2000; Simon and Makarewicz, 2009). In this study, the proportions of non-eroded area and severely loss area within orchard land were 44.4% and 16.9%, respectively, and both of them were greater than in arable land.

In conclusion, the PP loss within forestland was absolutely the slightest among three typical land use patterns. With respect to the other two land use patterns, the differences were not notable from figure 3, while the statistical data indicated that the mean loss amount in

Table 4. Statistical data of PP loss amount within three land use patterns in study site (*P<0.05*).

Land Use	Loss Amount (t/km²•a)				Loss Intensity Grades (%)			
	Min	Max	Mean	*Cv* (%)[a]	Non-eroded	Slightly	Moderate	Severest
Forestland	0	36.472	7.31	11.9	79.31	18.37	2.09	0.23
Arable land	2.33	110.78	25.75	23.3	32.76	30.65	20.55	16.04
Orchard	1.76	100.3	19.15	49.8	44.43	27.13	11.54	16.94

[a] *Cv* (%): Coefficient of variation.

arable land was slighter greater than in orchard (table 4), and the orchard land owned more non-eroded and severely loss region proportions. These results showed that although land use greatly affected PP loss, the influence cannot be oversimplified, especially with respect to arable land and orchard land.

CRITICAL UNDERLYING FEATURES FOR DIFFERENT PP LOSS GRADES

Various land use patterns greatly affected PP loss. However, the diversity of PP loss among different patterns was not simply linear. Moreover, the loss intensity also varied greatly within a single land use pattern. Therefore, the relative underlying surface features need to be identified to clarify the critical factors causing PP loss variations among different land use patterns. This may also be helpful in identifying the factors impacting on PP loss variations within single land use pattern. The selected underlying surface features included topography indicators, which were relatively stable, and several soil and vegetation indicators, which were influenced largely by anthropogenic activities.

The value range of topographical elements, including elevation and slope within different land use patterns and loss grades, are showed in table 5. Elevation was closely related with PP loss. The mean elevation exceeded 100 m within non-eroded area, with the maximum value reached 309 m. However, the mean elevation within the severest loss area was only 39.7 m. Similarly, the elevation of arable land and orchard land also varied widely in non-eroded area and severe loss area. All of the three land use patterns showed that the increased elevation, which was always accompanied by the slighter PP loss intensity. The results were partly due to the human encroachment and always occurred in plain areas, which is more likely to result in soil erosion and non-point source pollution.

Compared with elevation, the impact of slope feature on PP loss was relative indirect. With respect to forestland, the mean of slope was 10.58° and 16.92° for non-eroded area and severest loss area, respectively, indicating that the topography of severely loss region was slightly steeper than non-eroded area. However, the slope did not varied notable in arable land and orchard land. Obviously, the majority of the study area had little topographical relief. The slopes were similar in these two land use types, and consistently less than 20°. In the arable and orchard land, the mean value never exceeded 10°. Typically, the flat terrain area is suitable for human encroachment, and the slope was preferably less than 25°. A strong positive relationship was observed between slope and erosion intensity when the slope exceeded 25°. Our results showed that the slope were less than 20° in most cases except for a some small portion of forestland, inferring that the PP loss variation might be resulted from human encroachment including tillage, fertilization, pesticide application and mechanical cultivation. The influence of slope was probably minimal and insignificant when the slope was under 25°

Soil P concentration was also influenced by vegetation conditions and soil properties including SOM and soil mechanical composition. Therefore, the measured properties of totally 75 samples were also clustered by each land use type and PP loss grade (table 6).

A significant negative relationship was found between NDVI and PP loss, especially in orchard land. The differences among NDVI values were notable between non-eroded region and severe loss region. The maximum value of severe loss region was 0.332, which was close to the minimum value of non-eroded region. These results indicated that decreased tendency of NDVI always accompanied by aggravated PP loss intensity. Moreover, the Standard deviation of NDVI within orchard land was reached 0.09, much greater than the values within forestland and arable land, which values were tended to 0. This feature was consistent with the results that PP loss of orchard owned the highest spatial variability, and also further proved that diversified cropping pattern had a profound effect on PP loss (Wu et al., 2012).

Soil organic matter was closely related to P loss in arable land and forestland. In those areas, the conditions of overlapping PP loss value rarely occurred in non-erode and severely loss region. For instance, the forestland contained a higher SOM content (the mean content was 2.62 g/kg and the maximum value was 3.22 g/kg) than arable land and orchard land, and the maximum value was almost as much as the minimum value for non-eroded grade within forestland. In addition, although the SOM content in arable land was generally less than forestland, a similar tendency of increased PP loss with decreasing SOM concentration was observed. These results also indicated that the SOM can be designated as a critical indicator for PP loss within forestland and arable land. In contrast, TN concentration and PP loss seems not closely correlated. This probably resulted from that lower nitrogen used in fertilizer than phosphate in arable land and orchard land, and the nitrogen in soil was in a relative stable form when compared with Phosphate, which resulted in the nitrogen status changed not obvious when compared with the background status.

Table 5. Statistical data of topography features vs. PP loss grade and land use pattern.

Indicators		Arable Land		Forestland		Orchard Land	
		Non-Eroded	Severest Loss	Non-Eroded	Severest Loss	Non-Eroded	Severest Loss
Elevation (m)	Min	6.0	3.0	58	17	15.0	7.0
	Max	88.0	8.0	309	101	134	31.0
	Mean	19.0	3.71	113.94	39.71	27.77	11.94
	SD	9.66	1.93	38.53	11.44	11.33	5.44
Slope (°)	Min	0	0	4.417	3.258	0	0
	Max	12.46	8.85	25.78	32.68	17.10	12.53
	Mean	5.74	3.60	10.58	16.92	8.03	7.57
	SD	6.55	8.93	5.93	1.25	3.23	0.34

Table 6. Comparative data of soil properties and vegetation status vs. land use pattern and PP loss grade.

Indicators		Arable Land		Forestland		Orchard Land	
		Non-Eroded	Severest Loss	Non-Eroded	Severest Loss	Non-Eroded	Severest Loss
SOM (g/kg)	Min	1.88	0.52	2.87	1.38	0.51	0.32
	Max	3.70	2.05	5.59	3.22	3.12	2.64
	Mean	2.79	0.94	3.72	2.62	1.64	1.12
	SD	0.10	0.11	0.09	0.22	0.22	0.15
Sand (%)	Min	8.66	13.57	9.6	10.01	4.53	5.55
	Max	16.2	30.30	16.4	17.1	16.32	20.4
	Mean	10.32	24.33	12.24	12.88	10.22	13.58
	SD	1.02	3.44	1.77	0.98	3.98	1.99
Silt (%)	Min	69.5	62.5	70.2	72.9	69.2	67.6
	Max	80.7	71.6	77.2	76.1	71.1	74.1
	Mean	74.6	65.9	72.01	72.60	70.30	70.4
	SD	0.22	0.88	0.23	0.34	0.09	1.16
Clay (%)	Min	2.26	2.04	2.78	2.44	3.78	2.77
	Max	13.45.	11.48	15.52	10.02	11.11	7.94
	Mean	5.72	10.09	7.02	5.63	6.08	4.94
	SD	0.98	1.02	0.11	0.83	0.42	0.62
TN (g/kg)	Min	0.12	0.05	0.06	0.08	0.11	0.13
	Max	0.23	0.19	0.17	0.20	0.23	0.21
	Mean	0.173	0.08	0.11	0.11	0.08	0.11
	SD	0.02	0.04	0.06	0.08	0.11	0.08
NDVI	Min	0.456	0.090	0.602	0.387	0.290	0.083
	Max	0.877	0.774	0.862	0.668	0.760	0.332
	Mean	0.573	0.402	0.596	0.422	0.600	0.195
	SD	0.02	0.01	0.02	0.02	0.09	0.06

According to Gong et al. (2003), the silt proportion in Alfisols and Histic soils should exceed 78%. It is acknowledged that erosion intensity and PP loss amount increase as silt proportion decreases and sand proportion increases because the tiny particles of silt are prone to be displaced. Consequently, the surface soil simultaneously becomes rougher due to increased sand content (Montgomery et al., 1997; Luleva et al., 2011). Our results (table 6) showed consistent patterns with previously published data. In arable land, PP loss was closely related to soil composition; the high proportion of sand and low proportion of silt allowed this relationship to be more evident than those in forest land and orchard land (table 6). Moreover, the differences between non-eroded grade and severely loss grade were also significant (table 6), and the difference was most remarkably attributed to the proportions of sand and silt.

In plains and low hill areas, the topographical features such as slope did not directly affect PP loss status, while the elevation was strongly and negatively related to PP loss in all land use patterns, due to the elevation is directly related with the frequency of human activities. The soil properties including SOM and composition were key factors that influenced PP loss within arable land. Both SOM content and silt proportion were strongly and negatively related to PP loss, and the maximum value of SOM content and silt proportion could be designated as a threshold value and used to distinguish between severely loss region and other loss grades. Nevertheless, the NDVI index would be identified as the most critical factor related to PP loss within orchard land duo to its strong and negative relation to PP loss. The variation of NDVI was the highest in orchard land among the different land use patterns probably because of diverse crops grown in orchards. Therefore, it can be inferred that the PP loss within arable land was controlled by soil SOM and soil mechanical composition, and the status of these properties would be impacted by human encroachment, especially by fertilizer application, whereas the PP loss status within orchard land was mainly controlled by NDVI priority, which varied due to the different varieties of crops in the orchard land.

CONCLUSION

To better understand soil PP loss status under typical land use patterns, this study assessed the spatial characteristics of PP loss using solid pollutants loss model and based on high-resolution remote sense data source. Our results analyzed differences of PP loss intensity within each land use pattern, and clarified critical factors that affected PP loss from the following aspects such as terrain, vegetation s and soil properties. In general, PP loss in this area was moderate, the no-eroded grade and slightly-eroded grade covered most of the study area. PP loss varied significantly in different land use patterns. The forestland had the slightest PP loss among all land uses, whereas the arable land exhibited the highest loss intensity. The non-eroded region and severely loss region within orchard land accounted for higher proportions than those in arable land, which indicated that variations of PP loss intensity within orchard land were probably greater than those in arable land. The differences among different land use patterns might be partly due to differences in critical underlying factors. Specially, several soil properties including SOM and mechanical composition were identified as key factors for PP loss within arable land. The NDVI index, which varied significantly due to different cropping patterns, was the most critical negative factor of PP loss within orchard.

In conclusion, as NPS P loads survey by remote sensing and GIS is becoming more accessible, researchers should make full use of this technology for more accurate and

updated information. Moreover, a longer temporal sequence as well as a better quantification of seasonal and inter-annual nutrients loads is needed in order to provide more accurate information for the watershed management. In addition, rather than relying solely on historical data, updated soil properties and land use data are necessary for effective watershed pollution management.

ACKNOWLEDGEMENTS

This work was funded by the National Natural Science Foundation of China (41301227) and Research Fund of State Key Laboratory of Soil and Sustainable Agriculture, Nanjing Institute of Soil Science, Chinese Academy of Science (Y412201427).

Data were supported by Scientific Data Sharing Platform for Lake and Watershed, Nanjing Institute of Geography and Limnology, Chinese Academy of Sciences

REFERENCES

Beasley, D. B., Huggins, L. F., & Monke, E. J. (1980). Answers: A model for watershed planning. *Trans. ASAE, 23*(4), 938-944. http://dx.doi.org/10.13031/2013.34692

Bechmann, M., Stalnacke, P., Kvoerno, S., Eggestad, H. O., & Oygarden, L. (2009). Integrated tool for risk assessment in agricultural management of soil erosion and losses of phosphorus and nitrogen. *Sci. Total Environ., 407*(2), 749-759. http://dx.doi.org/10.1016/j.scitotenv.2008.09.016

Bu, Z. H., Yang, L. Z., Bu, Y. X., & Wu, J. Y. (2002). Soil erodibility (K) value and its application in Taihu lake catchment [in Chinese]. *Acta Pedologica Sinica, 39*(3), 296-300.

Castoldi, N., Bechini, L., & Stein, A. (2009). Evaluation of the spatial uncertainty of agro-ecological assessments at the regional scale: the phosphorus indicator in northern Italy. *Ecol. Indic., 9*(5): 902-912. DOI: 10.1016/j.ecolind.2008.10.009

Cheng, J. M., Song, T., & Li, Y. (2012). Estimation of nitrogen and phosphorus loading of agricultural non-point sources along Nansi Lake based on GIS [in Chinese]. *Res. Soil and Water Conserv., 19*(3), 284-288.

Cui, G.B., Zha, H.E., & Luo, J. (2003). Quantitative evaluation of Non-point Pollution of Taihu Watershed using Geographic Information System [in Chinese]. *J. Lake Sci., 15*(3), 236-244

Durigon, V. L., Carvalho, D. F., Antunes, M. A. H., Oliveira, P. T., & Fernandes, M. M. (2014). NDVI time series for monitoring RUSLE cover management factor in a tropical watershed. *Int. J. Remote Sens., 35*(2), 441-453. http://dx.doi.org/10.1080/01431161.2013.871081

Emili, L. A., & Greene, R. P. (2013). Modeling agricultural nonpoint source pollution using a geographic information system approach. *Environ. Manag., 51*(1), 70-95. http://dx.doi.org/10.1007/s00267-012-9940-4

Evanylo, G., Sherony, C., Spargo, J., Starner, D., Brosius, M., & Haering, K. (2008). Soil and water environmental effects of fertilizer-, manure-, and compost-based fertility practices in an organic vegetable cropping system. *Agr. Ecosyst. Environ.*,*127*(1-2), 50-58. http://dx.doi.org/10.1016/j.agee.2008.02.014

Ferro. (1997). Further remarks on a distributed approach to sediment delivery. *Hydrol. Sci. J., 42*, 633-647. DOI: 10.1080/02626669709492063

Fu, G. B., Chen, S. L., & McCool, D. K. (2006). Modeling the impacts of no-till practice on soil erosion and sediment yield with RUSLE, SEDD, and ArcView GIS. *Soil Tillage Res., 85*(1-2), 38-49. http://dx.doi.org/10.1016/j.still.2004.11.009

Gburek, W. J., & Sharpley, A. N. (1998). Hydrologic controls on phosphorus loss from upland agricultural watersheds. *JEQ, 27*(2), 267-277. http://dx.doi.org/10.2134/jeq1998.00472425002700020005x

Gburek, W. J., Sharpley, A. N., & Golmar, G. J. (2000). Critical areas of phosphorus export from agricultural watersheds. In A. N. Sharpley (Ed.), *Agriculture and phosphorus management: The Chesapeake Bay.* Boca Raton, FL: CRC.

Guo, H. Y., Wang. X. R., & Zhu, J. G. (2004). Quantification and Index of Non-Point Source Pollution in Taihu Lake Region with GIS. *Environ. Geochem. Hlth., 26*(2), 147-156. doi:10.1023/B:EGAH.0000039577.67508.76

Gong, Z. T., Chen, Z. C., & Zhang, G. L. (2003). World reference base for soil resources (WRB): Establishment and development [in Chinese]. *Soils, 35*(4), 271-278.

He, B., Oki, K., Wang, Y., Oki, T., Yamashiki, Y., Takara, K., ... Kawasaki, N. (2012). Analysis of stream water quality and estimation of nutrient load with the aid of Quick Bird remote sensing imagery. *Hydrol. Sci. J., 57*(5), 850-860. http://dx.doi.org/10.1080/02626667.2012.683792

Houba, V. J., Van der Lee, J. J., Novozamsky, I., & Walinga, I. (1989). Soil and plant analysis, a series of syllabi: Part 5. *Soil Analysis Procedures*. The Netherlands: Wageningen Agricultural University.

Jain, M. K., & Kothyari, U. C. (2000). Estimation of soil erosion and sediment yield using GIS. *Hydrol. Sci. J., 45*(5), 771-786. http://dx.doi.org/10.1080/02626660009492376

Laurent, F., & Ruelland, D. (2011). Assessing impacts of alternative land use and agricultural practices on nitrate pollution at the catchment scale. *J. Hydrol., 409*(1-2), 440-450. http://dx.doi.org/10.1016/j.jhydrol.2011.08.041

Li, H.-P. Huang, W. Y., Yang, G. S., & Liu, X. M. (2006). Non-point pollutant concentrations for different land uses in Lihw River watershed of Taihu Region [in Chinese]. *China Environ. Sci., 26*(6), 243-247.

Li, Z.-F., Yang, G.-S., & Li, H.-P. (2007). Estimation of nutrient export coefficient from different land use types in Xitiaoxi watershed [in Chinese]. *JSWC, 21*(1), 1-4.

Lin, C., He, M. C., Zhou, Y. X., Guo, W., & Yang, Z. F. (2008). Distribution and contamination assessment of heavy metals in sediment of the Second Songhua River, China. *Environ. Monit. Assess., 137*(1), 329-342. http://dx.doi.org/10.1007/s10661-007-9768-1

Luleva, M. I., Van der Werff, H., Jetten, V., & Van der Meer, F. (2011). Can infrared spectroscopy be used to measure change in potassium nitrate concentration as a proxy for soil particle movement? *Sensors, 11*(4), 4188-4206. http://dx.doi.org/10.3390/s110404188

McDowell, R. W., Sharpley, A. N., & Chalmers, A. T. (2002). Land use and flow regime effects on phosphorus chemical dynamics in the fluvial sediment of the Winooski River, VT. *Ecol. Eng., 18*(4), 477-487. http://dx.doi.org/10.1016/S0925-8574(01)00108-2

Montgomery, J. A., Busacca, A. J., Frazier, B. E., & McCool, D. K. (1997). Evaluating soil movement using Cesium-137 and the revised Universal Soil Loss Equation. *SSSAJ, 61*(2), 571-579. http://dx.doi.org/10.2136/sssaj1997.03615995006100020029x

Nash, J. E., & Sutcliffe, J. V. (1970). River flow forecasting through conceptual models. Part I: A discussion of principles. *J. Hydrol., 10*(3), 282-290. http://dx.doi.org/10.1016/0022-1694(70)90255-6

Norton, L., Elliott, J. A., Maberly, S. C., & May, L. (2012). Using models to bridge the gap between land use and algal blooms: An example from the Loweswater catchment, U.K. *Environ. Model. Software, 36*, 64-75. http://dx.doi.org/10.1016/j.envsoft.2011.07.011

Osborne, S. L., Schepers, J. S., Francis, D. D., & Schlemmer, M. R. (2002). Detection of phosphorus and nitrogen deficiencies in corn using spectral radiance measurements. *Agron. J., 94*(6), 1215-1221. http://dx.doi.org/10.2134/agronj2002.1215

Ouyang, W., Skidmore, A. K., Toxopeus, A. G., & Hao, F. H. (2010). Long-term vegetation landscape pattern with non point source nutrient pollution in upper stream of Yellow River basin. *J. Hydrol., 389*(3-4):373-80.

Ouyang, W., Huang, H., Hao, F., Shan, Y., & Guo, B. (2012). Evaluating spatial interaction of soil property with non-point source pollution at watershed scale: The phosphorus indicator in Northeast China. *Sci. Total Environ., 432*, 412-421. http://dx.doi.org/10.1016/j.scitotenv.2012.06.017

Shen, Z., Hong, Q., Chu, Z., & Gong, Y. (2011). A framework for priority non-point source area identification and load estimation integrated with APPI and PLOAD model in Fujiang watershed, China. *Agric. Water Manag., 98*(6), 977-989. http://dx.doi.org/10.1016/j.agwat.2011.01.006

Simon, R. D., & Makarewicz, J. C. (2009). Impacts of manure management practices on stream microbial loading into Conesus Lake, NY. *J. Great Lakes Res., 35, Suppl. 1*, 66-75. http://dx.doi.org/10.1016/j.jglr.2009.01.002

Smith, P. N. H., & Maidment, D. R., (1995). *Hydrologic data development system. CRWR Online Report No. 95-1.* Center for Research in Water Resources, University of Texas, Austin, TX.

Soil Science Society of China. (2000). *Methods of soil agrochemistry analysis* [in Chinese]. Beijing, China: Chinese Agric. Sci. Technol. Press.

Sridhar, B. B. M., Vincent, R. K., Witter, J. D., & Spongberg, A. L. (2009). Mapping the total phosphorus concentration of biosolid amended surface soils using LANDSAT TM data. *Sci. Total Environ., 407*(8), 2894-2899. http://dx.doi.org/10.1016/j.scitotenv.2009.01.021

Strauss, P., Leone, A., Ripa, M.M., Turpin, N., Lescot, J.M., & Laplana, R. (2007). Using critical source areas for targeting cost-effective best management practices to mitigate phosphorus and sediment transfer at the watershed scale. *Soil. Use. Manage., 23,* 144-153

Wang, X. L., Wang, Q., Wu, C. Q., Liang, T., Zheng, D., & Wei, X. (2012). A method coupled with remote sensing data to evaluate non-point source pollution in the Xin'anjiang catchment of China. *Sci. Total Environ., 430*, 132-143. http://dx.doi.org/10.1016/j.scitotenv.2012.04.052

Wischmeier, W. H., & Smith, D. D. (1978). *Predicting rainfall erosion losses.* USDA agricultural research services handbook 537. 57-58. Washington, DC: USDA.

Wu, L., Long, T.-Y, Liu, X., & Guo, J.-S. (2012). Impacts of climate and land-use changes on the migration of non-point source nitrogen and phosphorus during rainfall-runoff in the Jialing River watershed, China. *J. Hydrol., 475*, 26-41. http://dx.doi.org/10.1016/j.jhydrol.2012.08.022

Xu, L., Xie, Y., Fu, S.-H., Liu, B.-Y., Lu, B.-J., & Yuan, A.-P. (2007). Simple method of estimating rainfall erosivity under different rainfall amount of Beijing [in Chinese]. *Res. Soil and Water Conserv., 6*, 398-402.

Xu, L. F., Xu, X. G., & Meng, X. W. (2012). Risk assessment of soil erosion in different rainfall scenarios by RUSLE model coupled with Information Diffusion Model: A case study of Bohai Rim, China. *CATENA, 100*, 74-82. http://dx.doi.org/10.1016/j.catena.2012.08.012

Yang, L. X. (2009). Researches on characteristics and influencing factors of phosphorous loss in runoff in the typical land use of Taihu watershed. Zhejiang, China: Zhejiang University Press.

Yang, W. J., Cheng, H. G., Hao, F. H., Ouyang, W., Liu, S. Q., & Lin, C. Y. (2012). The influence of land-use change on the forms of phosphorus in soil profiles from the Sanjiang Plain of China. *Geoderma, 189-190*, 207-214. http://dx.doi.org/10.1016/j.geoderma.2012.06.025

Zhang, R., Liu, X., Heathman, G. C., Yao, X., Hu, X., & Zhang, G. L. (2013). Assessment of soil erosion sensitivity and analysis of sensitivity factors in the Tongbai-Dabie mountainous area of China. *CATENA, 101*, 92-98. http://dx.doi.org/10.1016/j.catena.2012.10.008

Zhang, X. Y., Huang, X. J., Zhao, X. F., Lu, R., & Lai, L. (2009). Impacts of land use change on the vegetation carbon storage in the region around Taihu Lake, China. *J. of Natural Resour., 24*(8), *1343-1353.*

Zhou, H. P., & Gao, C. (2008). Identifying critical source areas for non-point phosphorus loss in Chaohu watershed [in Chinese]. *Environ. Sci., 29*(10), 2696-2702.